Soliton propagation in tapered silicon core fibers

Anna C. Peacock

Optoelectronics Research Centre, University of Southampton, Southampton SO17 1BJ, UK (acp@orc.soton.ac.uk)

Received August 6, 2010; revised September 22, 2010; accepted October 1, 2010;
posted October 5, 2010 (Doc. ID 133051); published October 28, 2010

Numerical simulations are used to investigate soliton-like propagation in tapered silicon core optical fibers. The simulations are based on a realistic tapered structure with nanoscale core dimensions and a decreasing anomalous dispersion profile to compensate for the effects of linear and nonlinear loss. An intensity misfit parameter is used to establish the optimum taper dimensions that preserve the pulse shape while reducing temporal broadening. Soliton formation from Gaussian input pulses is also observed—further evidence of the potential for tapered silicon fibers to find use in a range of signal processing applications. © 2010 Optical Society of America

OCIS codes: 160.6000, 190.4370, 190.5530.

Silicon waveguides with nanoscale core dimensions are fast becoming one of the fundamental building blocks in the development of highly integrated optoelectronic architectures [1]. The high refractive index contrast between the silicon core and silica cladding allows for tight mode confinement in the subwavelength structures to enhance the nonlinear effects and tune the waveguide dispersion. The ability to tailor the waveguide properties is particularly important for soliton applications, where the nonlinear effects can be balanced via precise management of an anomalous group velocity dispersion (GVD) to reduce signal degradation. Although silicon possesses a large normal material dispersion, nanoscale waveguides typically exhibit an anomalous dispersion at 1.5 μm owing to the strong waveguide contribution. In this regime, soliton-like solutions, which nearly maintain their shape, have been shown to exist [2]. However, owing to the large linear and nonlinear losses associated with propagation in silicon, these soliton-like pulses experience broadening, even over short lengths [3]. Importantly, soliton solutions are of interest not only for high-speed optical interconnects but also for a range of nonlinear applications, including switching and supercontinuum generation.

Soliton broadening associated with linear loss during long-haul transmission in silica fibers is a problem that has been subject to numerous investigations [4–6]. A favored solution is based on dispersion compensation, where a decreasing dispersion profile is used to compensate for the decreasing power-dependent nonlinearity. This is typically achieved using a tapered fiber, where, in low-loss silica, the decreasing anomalous dispersion can be realized through small decreases in the core diameter such that the effect on the mode area is negligible [7]. In silicon, however, it is not obvious whether a similar tapering approach can be applied, as the linear loss is large, thus requiring a more dramatic change in dispersion, and there is the added influence of the nonlinear loss. Furthermore, owing to the tight mode confinement in these nanoscale waveguides, changes in the core diameter will alter the mode area, and hence the nonlinearity coefficient.

In this Letter, numerical simulations are used to investigate soliton-like propagation in tapered silicon core fibers with decreasing anomalous dispersion [8]. The simulations are based on a fiber geometry due to the ease with which the dispersion can be controlled [9]; however, the results will also be applicable to silicon-on-insulator ridge waveguides with appropriately tailored dispersion profiles. Solutions are searched for that preserve the hyperbolic secant profile in both the temporal and spectral domains as well as maintaining the initial pulse width. Although no formal soliton solutions have been found for propagation in silicon waveguides where the effects of two-photon absorption (TPA), free-carrier absorption (FCA), and free-carrier dispersion (FCD) must be included, this analysis will provide insight into the potential for tapered structures to be used to reduce loss-induced pulse broadening in such systems.

Propagation of an optical pulse in a silicon tapered fiber can be described by a modified form of the nonlinear Schrödinger equation [9,10]:

$$\frac{\partial A}{\partial z} = -\frac{i\beta_2(z)}{2}\frac{\partial^2 A}{\partial t^2} + \frac{\beta_3(z)}{6}\frac{\partial^3 A}{\partial t^3} + i\gamma(z)|A|^2 A - \frac{1}{2}(\sigma_f + \alpha_l)A, \tag{1}$$

where $A(z,t)$ is the pulse envelope and $\beta_2(z)$, $\beta_3(z)$, and $\gamma(z)$ are, respectively, the GVD, third-order dispersion, and nonlinearity parameters as functions of the taper distribution. The complex nonlinear parameter includes the effects of TPA and is defined as $\gamma(z) = k_0 n_2/A_{\text{eff}}(z) + i\beta_{\text{TPA}}/2A_{\text{eff}}(z)$, where n_2 is the Kerr coefficient and β_{TPA} is the TPA coefficient. The final two terms are the linear loss α_l and the free-carrier contribution $\sigma_f = \sigma(1 + i\mu)N_c$, where σ is the FCA coefficient, μ governs the FCD, and the free-carrier density N_c is determined by the rate equation [10]

$$\frac{\partial N_c(z,t)}{\partial t} = \frac{\beta_{\text{TPA}}}{2h\nu_0}\frac{|A(z,t)|^4}{A_{\text{eff}}^2} - \frac{N_c(z,t)}{\tau_c}, \tag{2}$$

where τ_c is the carrier lifetime.

The parameters appearing in Eqs. (1) and (2) depend on the core material and size as well as the input pulse wavelength, which is chosen to be $\lambda_0 = 1.55$ μm. For convenience, a crystalline core is assumed, as the material parameters are well documented. The refractive indices of silicon and silica are calculated using the Sellmeier relations [11,12], and realistic values for the remaining material parameters are $n_2 = 6 \times 10^{-18}$ m^2/W, $\beta_{\text{TPA}} = 5 \times 10^{-12}$ m/W, $\tau_c \sim 1$ ns, $\alpha_l = 1$ dB/cm, $\sigma = 1.45 \times 10^{-21}$ m^2, and $\mu = 2k_c k_0/\sigma$ with $k_c = 1.35 \times 10^{-27}$ m^3 [10,13]. The dispersion and nonlinearity parameters as functions

of the taper core diameters are established via full-vector finite-element method analysis of the fundamental mode. Figures 1(a) and 1(b) show the GVD and effective mode area, respectively, over the anomalous dispersion range 480–920 nm in the silicon core fiber, from which $\beta_3(z)$ and $\gamma(z)$ can be obtained. It should be noted that in contrast to silica fibers, in a silicon taper the magnitude of the anomalous dispersion decreases for an increasing core size until crossing over to the normal dispersion regime at a diameter of ~920 nm. Although this means that as the dispersion decreases to compensate for the loss, the nonlinearity coefficient also decreases; importantly, the TPA-induced nonlinear loss decreases as well. The overall result is that, except for the linear loss, all the terms in Eq. (1) decrease, so that the soliton balance will depend on the relative rates of change of the parameters.

The exact form of the longitudinally varying dispersion and nonlinearity profiles will depend on the length and shape of the taper. As typical silicon device lengths are of the order of millimeters to centimeters only, exponential taper shapes will be considered [14], which is coincidentally the profile used for long-haul loss compensation in silica tapered fibers [6,7]. Thus, by fixing the taper length, the propagation will be defined by the input D_{in} and output D_{out} taper diameters. To establish whether soliton-like propagation is possible, the silicon taper length is first fixed to $L = 10$ mm and the pulse evolution is mapped as a function of the input and output taper diameters. Solutions are searched for that maintain the initial hyperbolic secant profile and starting width T_0, while the peak power $P(z)$ scales due to the losses, so that the pulse evolves as $U(z,t) = \sqrt{P(z)}\text{sech}(t/T_0)$. As a means of monitoring the pulse evolution, an rms intensity misfit parameter ε_I is defined in the usual form [15]:

$$\varepsilon_I(z) = \left\{\frac{1}{N}\sum_{j=1}^{N}[|A(z,t_j)|^2 - |U(z,t_j)|^2]^2\right\}^{1/2}. \quad (3)$$

For an input peak power $P_0 = 1$ W, the taper dimensions that best preserve both the shape and width to minimize the variation in $\varepsilon_I(z)$ are $D_{\text{in}} = 640$ nm and $D_{\text{out}} = 850$ nm, and the normalized evolution is shown in Fig. 2(a). The solid curve in Fig. 2(b) shows the evolution of the FWHM pulse width in closer detail, and the output peak power is 0.71 W. From the FWHM plot, it can be seen that although the pulse width increases slightly in the first half of the taper, it decreases in the second half to remain largely unchanged. This behavior is attributed to the exponentially decreasing taper profile not being the optimum shape, and future investigations will look to establish the profile that minimizes this deviation. Nevertheless, by comparing the evolution with that in an untapered fiber with the same starting diameter so that the input soliton parameters are unchanged (dashed curve), the effects of pulse broadening in the untapered structure is clear and the output peak power is correspondingly reduced to 0.63 W. To better understand the relative influence of the linear and nonlinear loss contributions in the silicon taper, the evolution is also plotted with no loss (dashed-dotted curve) and for linear loss only (solid circles), with both cases now showing the expected decrease in the pulse width. The relative contribution of the nonlinear loss can then be determined, from which it can be observed how the strong nonlinear loss during the initial stages of the propagation affects the overall evolution.

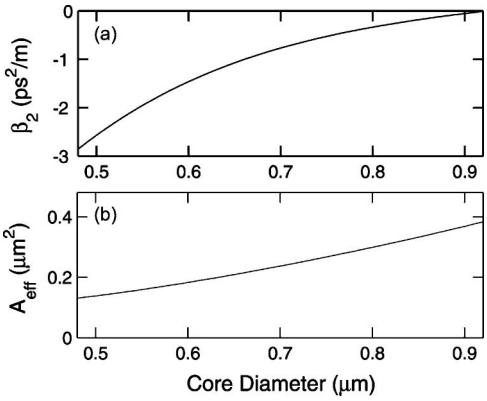

Fig. 1. (a) GVD and (b) effective mode area as functions of the silicon fiber core diameter.

Likewise, a similar analysis can be conducted for any desired taper length considered reasonable given the value of the linear loss. For the material and pulse parameters used in Figs. 2(a) and 2(b), solutions that maintain their shape and width have been found over the range $L = 2$–20 mm. In particular, for a waveguide length of 20 mm, the taper dimensions that minimize the variation in $\varepsilon_I(z)$ are $D_{\text{in}} = 600$ nm and $D_{\text{out}} = 900$ nm. The corresponding FWHM evolution is shown in Fig. 2(c) (solid curve), which is again compared to that for an untapered fiber with the same starting diameter (dashed curve). Furthermore, as the optimum taper dimensions depend on the starting peak power, this length range can be extended by simply varying the choice of P_0.

To evaluate the degree to which the pulses have maintained their soliton-like form, Fig. 3 plots the output (a) temporal and (b) spectral profiles of the pulse in Fig. 2(a), following 10 mm of propagation, together with their hyperbolic secant fits (circles). The slight asymmetry seen in the outputs is primarily due to the effects of β_3; however, there is still excellent agreement

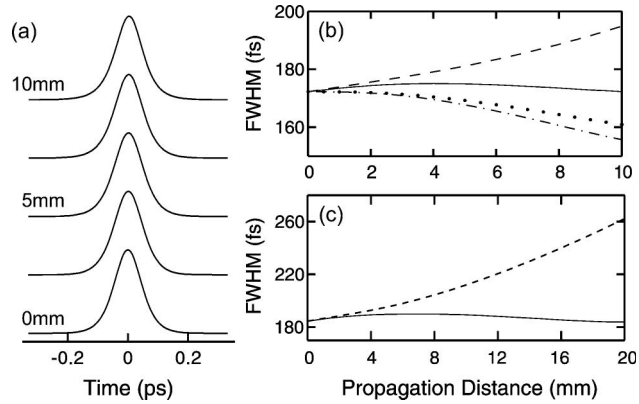

Fig. 2. Soliton evolution in a 10 mm taper: (a) normalized profiles and (b) FWHM (solid curve) compared to an untapered fiber (dashed curve), taper with no loss (dashed-dotted curve), and taper with linear loss (circles). (c) FWHM over 20 mm in a taper (solid curve) and an untapered fiber (dashed curve).

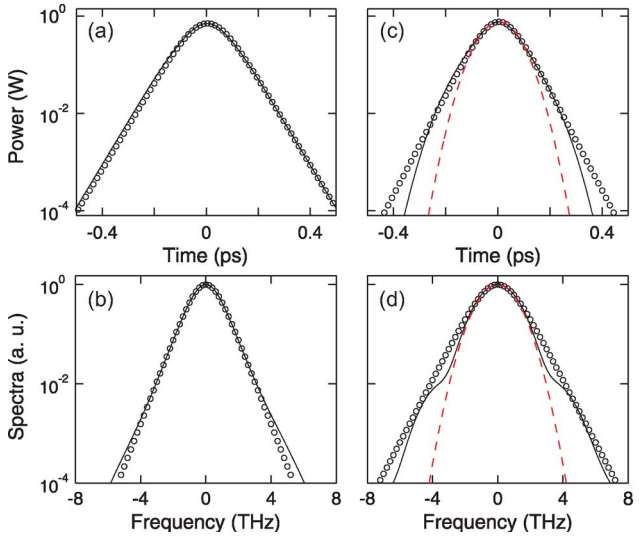

Fig. 3. (Color online) (a) Temporal and (b) spectral profiles following soliton propagation in a silicon taper (solid curves); hyperbolic secant fits (circles). (c) and (d) Outputs following soliton formation from a Gaussian input pulse (solid curve), hyperbolic secant (circles), and Gaussian (dashed curve) fits.

with the fits in both domains. Calculating the temporal intensity misfit at the output from the taper yields $\varepsilon_I(L) = 0.0013$. The value of this misfit can be quantified by comparing it to the misfit calculated for the output from the untapered fiber $\varepsilon_I(L) = 0.0038$ [Fig. 2(b) dashed curve], which is three times larger. Similarly, calculating the intensity misfits for the output pulses after 20 mm of propagation, as given in Fig. 2(c), the tapered output yields $\varepsilon_I(L) = 0.0014$, more than five times smaller than that of the untapered output $\varepsilon_I(L) = 0.0075$.

To demonstrate the robustness of these soliton-like solutions, additional simulations have been conducted to investigate the formation of solitons from nonoptimum input pulses during propagation in a silicon taper. Such soliton formation has already been observed experimentally in an untapered nanoscale silicon waveguide [2]. Figures 3(c) and 3(d) show the output pulse and spectrum, respectively, from the silicon taper generated via propagation of a Gaussian input with the same P_0 and FWHM pulse duration as the soliton input from Fig. 3(a). Comparing this pulse with both Gaussian (dashed curves) and hyperbolic secant fits (circles), it is clear that the pulse is evolving toward the soliton shape, with the slight deformation seen in the spectrum being due to the increasing energy in the wings [2]. Further evidence for soliton formation is provided through the observation that the spectrum narrows during its transformation to the soliton shape and via the reduction in the intensity misfit from the input $\varepsilon_I(0) = 0.0035$ to the output $\varepsilon_I(L) = 0.0018$. Extensive simulations have also shown that soliton formation is fairly resilient to variations in the input pulse width and peak power, so that for changes in the optimum values of up to $\pm 40\%$, the pulse will still converge to a hyperbolic secant shape. However, it is important to note that as soliton formation is a nonlinear process, if the power is too low then the pulse will retain its Gaussian shape, while if it is too high it will undergo spectral broadening.

In conclusion, soliton-like propagation has been proposed in tapered silicon core fibers where the decreasing anomalous dispersion profile acts to compensate for the loss-induced pulse broadening. Numerical simulations have identified a range of realistic taper parameters over which soliton propagation and formation can occur, and the solutions are found to tolerate variations in the input pulse parameters. These results are expected to be of particular importance for applications where high-data-rate nonlinear optoelectronic devices are required.

The author holds a Royal Academy of Engineering fellowship and acknowledges the Engineering and Physical Sciences Research Council (EPSRC) (EP/G051755/1) for financial support and N. Healy for helpful discussions.

References

1. M. Lipson, Nanotechnol. **15**, S622 (2004).
2. J. Zhang, Q. Lin, G. Piredda, R. W. Boyd, G. P. Agrawal, and P. M. Fauchet, Opt. Express **15**, 7682 (2007).
3. L. Yin, Q. Lin, and G. P. Agrawal, Opt. Lett. **31**, 1295 (2006).
4. Y. Kodama and A. Hasegawa, Opt. Lett. **7**, 339 (1982).
5. A. Hasegawa, Opt. Lett. **8**, 650 (1983).
6. K. Tajima, Opt. Lett. **12**, 54 (1987).
7. A. J. Stentz, R. W. Boyd, and A. F. Evans, Opt. Lett. **20**, 1770 (1995).
8. N. Healy, J. R. Sparks, P. J. A. Sazio, J. V. Badding, and A. C. Peacock, Opt. Express **18**, 7596 (2010).
9. A. Peacock and N. Healy, Opt. Lett. **35**, 1780 (2010).
10. L. Yin and G. P. Agrawal, Opt. Lett. **32**, 2031 (2007).
11. H. H. Li, J. Phys. Chem. Ref. Data **9**, 561 (1980).
12. G. P. Agrawal, *Nonlinear Fiber Optics*, 2nd ed. (Academic, 1995).
13. R. A. Soref and B. R. Bennett, IEEE J. Quantum Electron. **23**, 123 (1987).
14. R. P. Kenny, T. A. Birks, and K. P. Oakly, Electron. Lett. **27**, 1654 (1991).
15. D. N. Fittinghoff, K. W. DeLong, R. Trebino, and C. L. Ladera, J. Opt. Soc. Am. B **12**, 1955 (1995).